Long-range surface plasmon polaritons at THz frequencies in thin semiconductor layers

(Invited Paper)

Yichen Zhang[1], **Audrey Berrier**[1], **and Jaime Gómez Rivas**[1,2*]

[1]*FOM Institute for Atomic and Molecular Physics, c/o Philips Research, High-Tech Campus 4, 5656 AE Eindhoven, The Netherlands*

[2]*COBRA Research Institute, Eindhoven University of Technology, P.O. Box 513, 5600 MB Eindhoven, The Netherlands*

[*]*Corresponding author: rivas@amolf.nl*

Received July 25, 2011; accepted September 5, 2011; posted online October 18, 2011

We present a theoretical investigation of THz long-range surface plasmon polaritons propagating on thin layers of InSb. The metallic behavior of doped semiconductors at THz frequencies allows the excitation of surface plasmon polaritons with propagation and confinement lengths that can be actively controlled. This control is achieved by acting on the free carrier density, which can be realized by changing the temperature of InSb.

OCIS codes: 240.6680, 300.6495.
doi: 10.3788/COL201109.110014.

Surface plasmon polaritons (SPPs) are electromagnetic waves coupled to the free charge carriers at the interface between a metal and a dielectric[1]. These waves propagate along the interface, while decaying evanescently away from it. The propagation length of SPPs is mainly limited by Ohmic losses in the metal. A possible way to lower these losses is to reduce the penetration of the electromagnetic field inside the metal, which can be achieved by coupling the SPPs at the opposite sides of a thin metallic film. These coupled SPPs are known as long-range surface plasmon polaritons (LRSPPs) and have been thoroughly investigated at optical frequencies in thin layers of noble metals[2].

In this letter, we present a theoretical investigation of LRSPPs at THz frequencies. The generation of THz radiation with short optical pulses in InSb has been reported in literature[3−5]. Also THz plasmonics with InSb structures has been proposed and investigated in various systems such as hole arrays[6], gratings[7−9], slits[10,11], slot cavities[12], and plasmonic antennas[13]. InSb behaves as a metal at THz frequencies, i.e., it has a negative real component of the permittivity. This behavior can be tuned by modifying the number of excited electrons into the conduction band, i.e., the free carrier density. We investigate here thin films (relative to THz wavelengths) of crystalline indium antimonide (InSb) embedded in quartz and propose a simple way to control the characteristic lengths of LRSPPs by changing the temperature of the semiconductor. Active control of SPPs represents one of the paradigms of current research on plasmonics.

Figure 1(a) displays the real (solid curve) and imaginary (dashed curve) components of the permittivity of InSb at 290 K. These values have been obtained using a Drude model for free electrons and values of the effective mass and mobility reported in literature[14]. Intrinsic InSb is a narrow gap semiconductor with a bandgap energy of 0.17 eV. At room temperature, there is a significant fraction of thermally excited electrons in the conduction band ($N \simeq 2 \cdot 10^{16}$ cm^{-3}) with high mobility ($\mu \simeq 7.7 \cdot 10^4$ cm^2/(V·s)), which provide a metallic character to InSb at low frequencies. This character can be appreciated by the negative real component of the permittivity at frequencies lower than the plasma frequency of InSb, i.e., $\omega \leqslant 2.8$ THz at 290 K. The density of thermally excited carriers and the permittivity of InSb can be controlled by changing the temperature in the semiconductor. Figure 1(b) displays the real (solid curve) and imaginary (dashed curve) components of the permittivity of InSb at 1 THz as a function of temperature. The inset represents the dependence of the free-carrier density with temperature: lowering the temperature reduces the free carrier density. Since the plasma frequency of a conductor scales with the root square of the carrier density, it shifts to lower frequencies as the temperature is reduced. The plasma frequency of InSb is around 1 THz for a temperature of 200 K. At lower temperatures the real component of the permittivity becomes positive and InSb behaves as a dielectric. Ohmic losses, characterized by the imaginary component of the permittivity, are also reduced as the temperature is lowered.

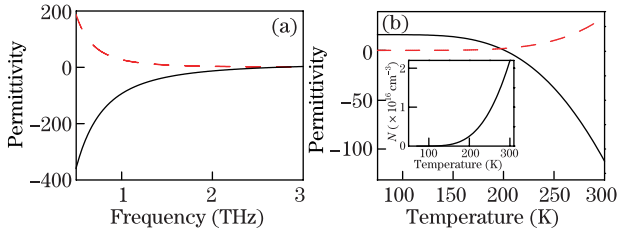

Fig. 1. Real (solid curve) and imaginary (dashed curve) components of the permittivity of InSb (a) at 290 K as a function of the frequency and (b) at 1 THz as a function of the temperature. The inset shows the dependence of the free charge carrier density in InSb with temperature.

An interface separating a metal from a dielectric supports SPPs. The dispersion relation of these surface modes can be derived by solving Maxwell equations at the interface and it is given by

$$k_{\rm spp} = \frac{\omega}{c}\sqrt{\frac{\epsilon_{\rm c}\epsilon_{\rm d}}{\epsilon_{\rm c}+\epsilon_{\rm d}}}, \tag{1}$$

where ω is the angular frequency, c is the speed of light in vacuum, and $\epsilon_{\rm c}$ and $\epsilon_{\rm d}$ are the permittivities of the conductor and the dielectric, respectively. Note that $k_{\rm spp}$ is a complex wavenumber due to the complex permittivity of the conductor. The solid curve in Fig. 2(a) represents the real component of the wavenumber of SPPs on an InSb-quartz interface at 290 K. The dashed area corresponds to the light cone or the allowed frequencies and wavenumbers for free space radiation in quartz. Surface modes are characterized by a wavenumber larger than that of free space radiation. In the case of a low-loss conductor, i.e., when the absolute value of the real component of the permittivity is much larger than the imaginary component, this characteristic behavior of SPPs is found at frequencies lower than the surface plasmon polariton frequency. This frequency is given by $\omega_{\rm spp} = \omega_{\rm p}/(\sqrt{\epsilon_\infty + \epsilon_{\rm d}})$, where $\omega_{\rm p}$ is the plasma frequency and ϵ_∞ is the contribution to the permittivity of bounded charges in the semiconductor. We also see in Fig. 2(a) that the separation of the wavenumber from the light cone increases at higher frequencies, reaching a maximum at approximately $\omega_{\rm spp}$ before folding into the light cone. The increased separation is the result of the better field confinement of SPPs to the surface. As a consequence of the lager field confinement, losses also become more important. The losses are proportional to the imaginary component of the SPPs wavenumber, which is displayed in Fig. 2(b) with the solid curve for frequencies lower than $\omega_{\rm spp}$.

The dispersion of SPPs is modified in thin metallic layers. In this system, SPPs at opposite sides of the thin film can couple with each other forming the so-called long-range and short-range SPPs (LRSPPs and SRSPPs). These coupled SPPs have different surface charge and field symmetries with respect to the middle plane of the thin layer. Similar to SPPs on single interfaces, the dispersion relation of LRSPPs and SRSPPs is obtained by solving Maxwell equations and applying the boundary conditions at the interfaces[15]. If the dielectric is the same at both sides of the thin film, we find the following dispersion relations:

$$\tanh({\rm i}k_{\rm z_c}d/2) = -\frac{\epsilon_{\rm c}k_{\rm z_d}}{\epsilon_{\rm d}k_{\rm z_c}}\ , \tag{2}$$

$$\tanh({\rm i}k_{\rm z_c}d/2) = -\frac{\epsilon_{\rm d}k_{\rm z_c}}{\epsilon_{\rm c}k_{\rm z_d}}\ , \tag{3}$$

for LRSPPs (Eq. (2)) and SRSPPs (Eq. (3)), respectively. In these equations, d is the thickness of the thin layer, and $k_{\rm z_c}$ ($k_{\rm z_d}$) are the wavenumbers in the direction normal to the thin layer in the conductor (dielectric). These wavenumbers are related to the wavenumber in the propagation direction $k_{\rm spp}$ by

$$k_{\rm spp}^2 + k_{\rm z_d}^2 = \epsilon_{\rm d}\frac{\omega^2}{c^2}, \tag{4}$$

$$k_{\rm spp}^2 + k_{\rm z_c}^2 = \epsilon_{\rm c}\frac{\omega^2}{c^2}. \tag{5}$$

Equations (2), (3), (4), and (5) can be solved numerically to obtain the complex wavenumbers as a function of the frequency. The complex wavenumber of LRSPPs and SRSPPs for a 10-μm thick layer of InSb at 290 K embedded in quartz are plotted in Figs. 2(a) and (b) as a function of the frequency with dashed and dotted curves, respectively. The dispersion of LRSPPs gets closer to the light cone than that of SRSPPs, which can be interpreted as a weaker confinement of the electromagnetic field to the thin layer and the concomitant reduction of losses. Indeed, as a consequence of the reduced losses, the imaginary component of the wavevector of LRSPPs is smaller than that of SPPs and SRSPPs. In the following we will focus on the characteristics of LRSPPs.

Figure 3 displays the (a) real and (b) imaginary components of the wavenumber of LRSPPs in a thin InSb layer surrounded by quartz, at a temperature of 210 K and at 1 THz as a function of the layer thickness. The wavenumbers in Fig. 3 are normalized to the wavenumber in quartz. For large thicknesses, the wavenumber converges to the value of SPPs on a single interface since the coupling of SPPs at the opposite side of the layer is negligible in this limit. When the thickness of the layer is reduced, the coupling increases and the values of the real and imaginary components of the wavenumber are reduced. The real component converges to the value of the wavenumber in quartz, while the imaginary component vanishes. This behavior is consistent with the interpretation of an electromagnetic field extending into the

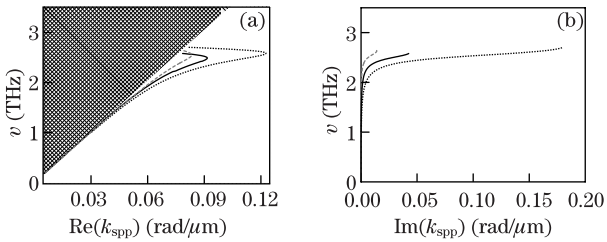

Fig. 2. (a) Dispersion relation of SPPs (solid curve), LRSPPs (dashed curve), and SRSPPs (dotted curved) on an InSb-quartz interface for a 10-μm-thick film of InSb surrounded by quartz. The dashed area represents the light cone in quartz. (b) Imaginary components of the wavenumber of SPPs (solid curve), LRSPPs (dashed curve), and SRSPPs (dotted curve) as a function of the frequency and for frequencies below the surface plasmon polariton frequency.

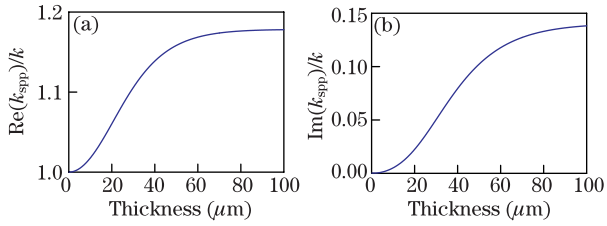

Fig. 3. (a) Real and (b) imaginary components of the wavenumber of LRSPPs, normalized by the wavenumber in quartz, in a InSb layer surrounded by quartz as a function of the thickness of the layer. The calculations correspond to a temperature of 210 K and a frequency of 1 THz.

surrounding dielectric and with a reduced energy density inside the thin absorbing layer.

The propagation (L_x) and confinement (L_z) lengths of LRSPPs are defined as the lengths over which the field intensity decreases by a factor of $1/e$ in the propagation direction and in the direction normal to the layer, respectively. These lengths are given by $L_x = 1/[2\mathrm{Im}(k_{spp})]$ and $L_z = 1/[2\mathrm{Im}(k_{z_d})]$[1]. Figure 4 displays L_x and L_z at 1 THz, normalized by the wavelength of free space radiation in quartz, as a function of the temperature in the range 210−290 K for LRSPPs in a 10-μm layer of InSb. As the temperature is reduced the normalized confinement length decreases by a factor of 1.75. Also losses increase at lower temperatures as a consequence of the better confinement of the field to the absorbing layer. In the temperature range 210−250 K the normalized propagation length of LRSPPs varies by almost a factor of 7. The small reduction of the propagation length for temperatures higher than 250 K can be understood by the increase of the imaginary component of the permittivity (see Fig. 1(b)). For temperatures below 210 K, InSb behaves as a dielectric at 1 THz. The large variation of the characteristic lengths of LRSPPs in InSb with modest variations in the carrier density, induced by changes in temperature, opens the possibility for active plasmonic circuits at THz frequencies. It should be pointed out that the changes in carrier density can be also induced by means of optical excitation of carriers. Reference [16] reported the switching of the SPPs transmission through an InSb Bragg mirror with a continuous wave laser and power densities on the order of a few W/cm^2. Optical

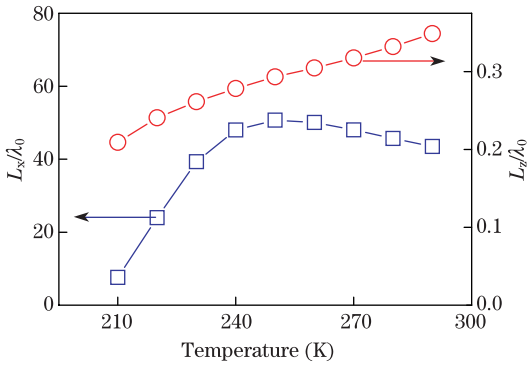

Fig. 4. Propagation length L_x (open squares) and decay length L_z (open circles) of LRSPPs in a thin layer of InSb surrounded by quartz as a function of the temperature, normalized by the wavelength in vacuum. The thickness of the InSb layer is 10 μm.

generation of carriers in semiconductors will allow the development of ultra-fast active plasmonic devices[17].

In conclusion, we present a theoretical study of the dispersion and characteristic lengths of long-range surface plasmon polaritons at THz frequencies in thin layers of InSb. These characteristic lengths can be controlled by changing the temperature of the semiconductor, i.e., by changing the density of thermally excited carriers.

This work was supported by the European Research Council (ERC) (No. 259272), the European Commission Seventh Framework Programme (FP7) (No. FP7-224189), and it is part of the research program of FOM, which is financially supported by NWO.

References

1. H. Raether, *Surface Plasmons* (Springer, Berlin, 1988).
2. P. Berini, Adv. Opt. Phot. **1,** 484 (2009).
3. B. B. Hu, X.-C. Zhang, and D. Auston, Appl. Phys. Lett. **57,** 2629 (1990).
4. S. C. Howells, S. D. Herrera, and L. A. Schlie, Appl. Phys. Lett. **65,** 2946 (1994).
5. P. Gu, M. Tani, S. Kono, K. Sakai, and X.-C. Zhang, J. Appl. Phys. **91,** 5533 (2002).
6. J. Gómez Rivas, C. Janke, P. Haring-Bolivar, and H. Kurz, Opt. Express **13,** 847 (2005).
7. J. Gómez Rivas, M. Kuttge, H. Kurz, P. Haring-Bolivar, and J. A. Sánchez-Gil, Appl. Phys. Lett. **88,** 082106 (2006).
8. R. Parthasarathy, A. Bykhovski, B. Gelmont, T. Globus, N. Swami, and D. Woolard, Phys. Rev. Lett. **98,** 153906 (2007).
9. M.-K. Chen, Y.-C. Chang, C.-E Yang, Y. Guo, J. Mazurowski, S. Yin, P. Ruffin, C. Brantley, E. Edwards, and C. Luo, Microwave Opt. Tech. Lett. **52,** 979 (2010).
10. X. Y. He and J. C. Cao, Commun. Theor. Phys. **49,** 485 (2008).
11. T. H. Isaac, J. Gómez Rivas, J. R. Sambles, W. L. Barnes, and E. Hendry, Phys. Rev. B **77,** 113411 (2008).
12. J. Li and K. J. Webb, J. Appl. Phys. **106,** 124901 (2009).
13. V. Giannini, A. Berrier, S. A. Maier, J. A. Sanchez-Gil, and J. Gómez Rivas, Opt. Express **18,** 2797 (2010).
14. S. Adachi, *Handbook on Physical Properties of Semiconductors* (Springer, Berlin, 2004).
15. R. Fuchs, K. L. Kliewer, and W. J. Pardee, Phys. Rev. **150,** 589 (1966).
16. J. Gómez Rivas, J. A. Sánchez-Gil, M. Kuttge, P. Haring Bolivar, and H. Kurz, Phys. Rev. B **74,** 245324 (2006).
17. A. Berrier, R. Ulbricht, M. Bonn, and J. Gómez Rivas, Opt. Express **18,** 23226 (2010).